Supplement of Biogeosciences, 21, 5393–5406, 2024
https://doi.org/10.5194/bg-21-5393-2024-supplement

Biogeosciences
Open Access

Supplement of

Cropland expansion drives vegetation greenness decline in Southeast Asia

Ruiying Zhao et al.

Correspondence to: Ruiying Zhao (ruiying@nus.edu.sg) and Xiangzhong Luo (xzluo.remi@nus.edu.sg)

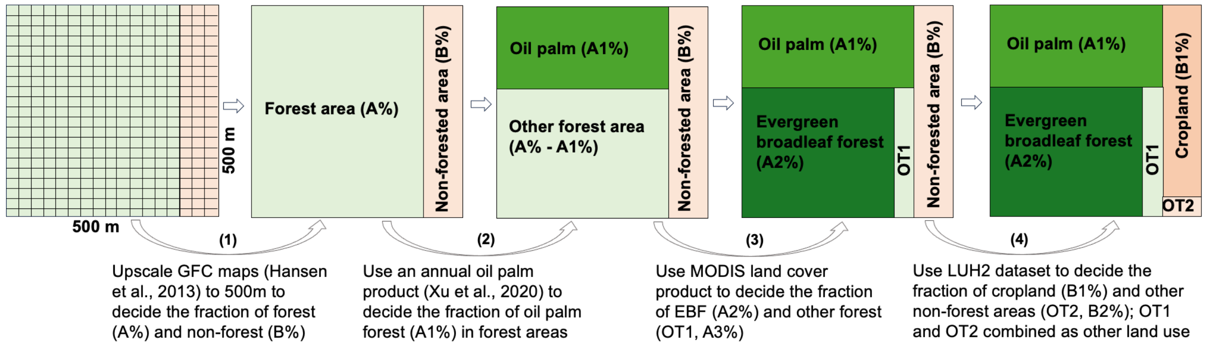

Figure. S1: A conceptual diagram illustrating the harmonization of land cover datasets within a 500-meter grid for this study. Step (1) involves upscaling fine-resolution Global Forest Change (GFC) maps to 500 meters to classify forest (A%) and non-forest (B%) areas. Steps (2) and (3) calculate the proportions of oil palm, evergreen broadleaf forest (EBF), and other forest types (OT1) within the forested areas. Oil palm percentages are derived from a 100-meter resolution product, upscaled to 500 meters, while EBF and OT1 are sourced from the MODIS dataset. Step (4) calculates cropland and other land uses (OT2) using the LUH2 dataset, with the assumption that LUH2 data at a 0.25° resolution applies to the 500-meter grid cells within each 0.25° grid. The conceptual figure illustrates only the fraction of each land use, not their specific locations.

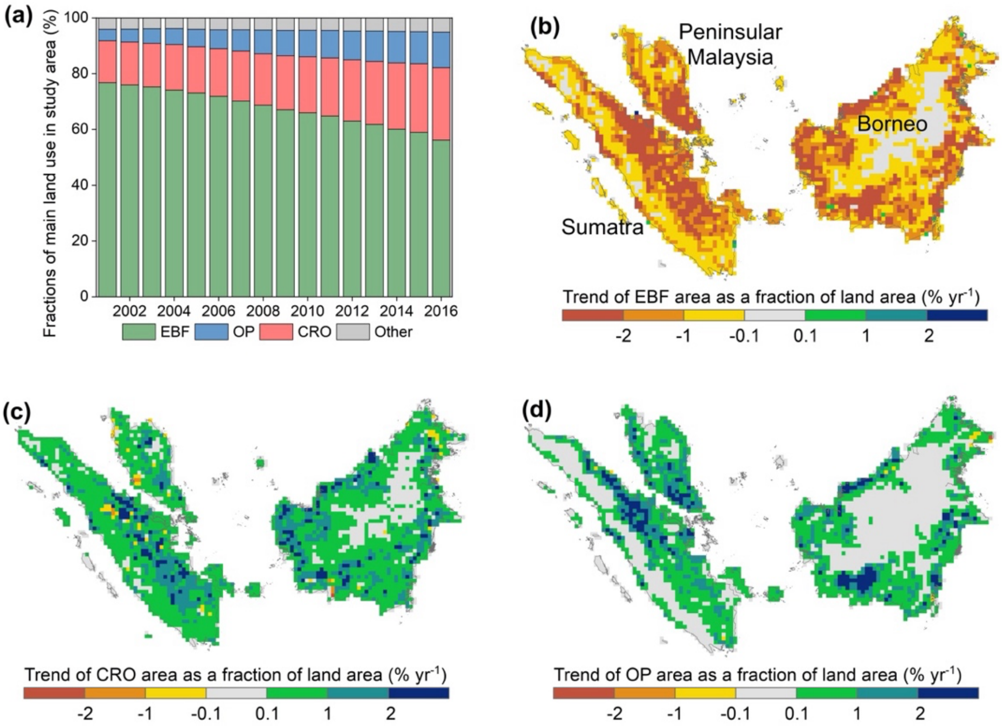

Figure S2: Land use composition and its changes from 2001 to 2016 in the study area, analyzed at a 0.25-degree resolution.

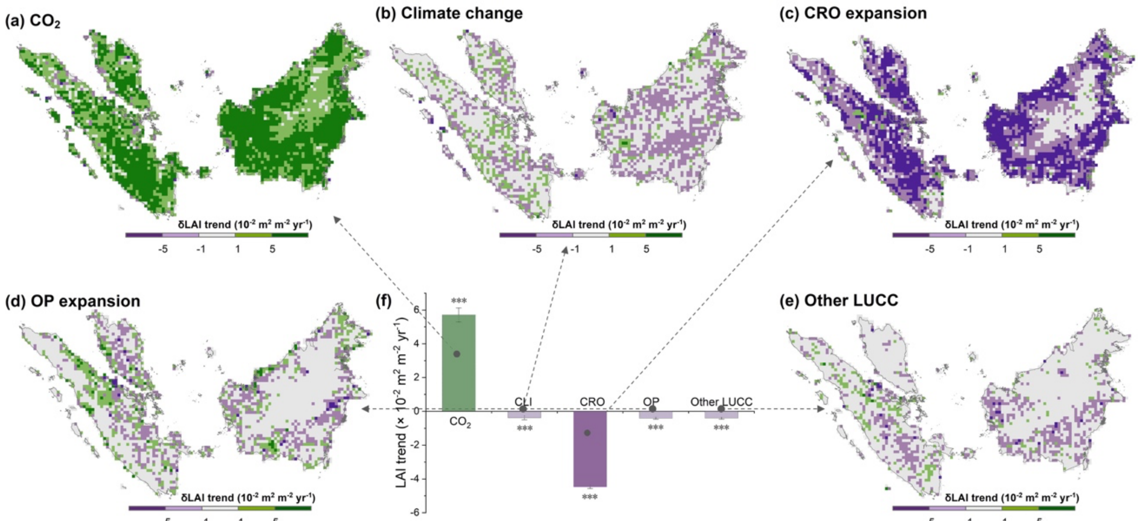

Figure S3: The spatial distribution of the pixel-wise impacts of each process on the greening trends, analysed at a 0.25-degree resolution.

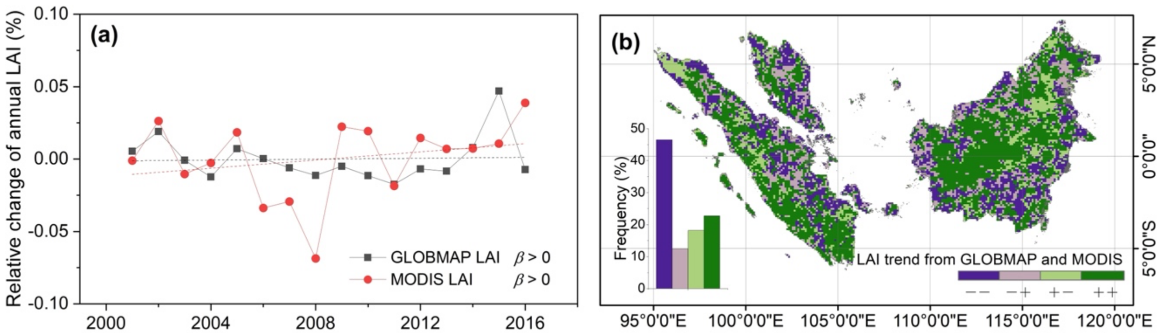

Figure S4: Comparison of LAI Trends Between MODIS and GLOBEMAP LAI Datasets. (a) illustrates the relative changes in annual mean LAI across the entire region from 2001 to 2016. (b) provides a spatial comparison of the datasets, where '++' denotes an increasing trend observed in both datasets, '−−' indicates a decreasing trend in both, '+−' signifies an increasing trend in GLOBEMAP but a decrease in MODIS, and '−+' represents the opposite scenario.

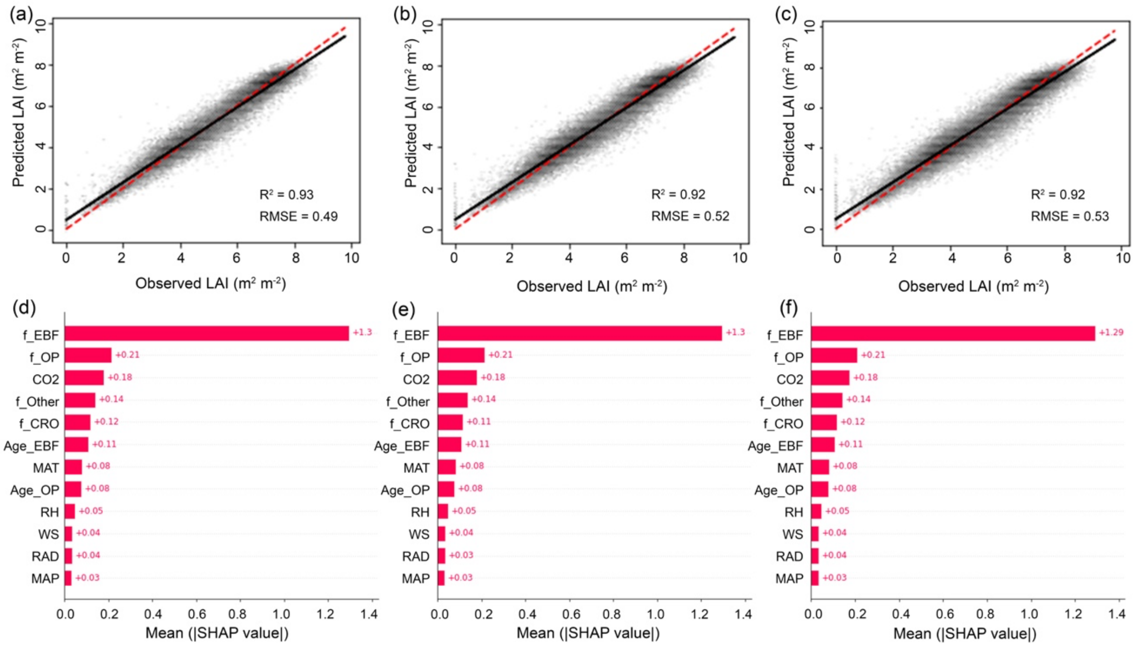

Figure S5: The impact of different training and testing dataset splitting ratios on model performance and interpretations. Panels (a) and (d) depict results using an 80%:20% ratio for training and testing, respectively. Panels (b) and (e) correspond to a 70%:30% ratio, while panels (c) and (f) reflect a 60%:40% ratio.

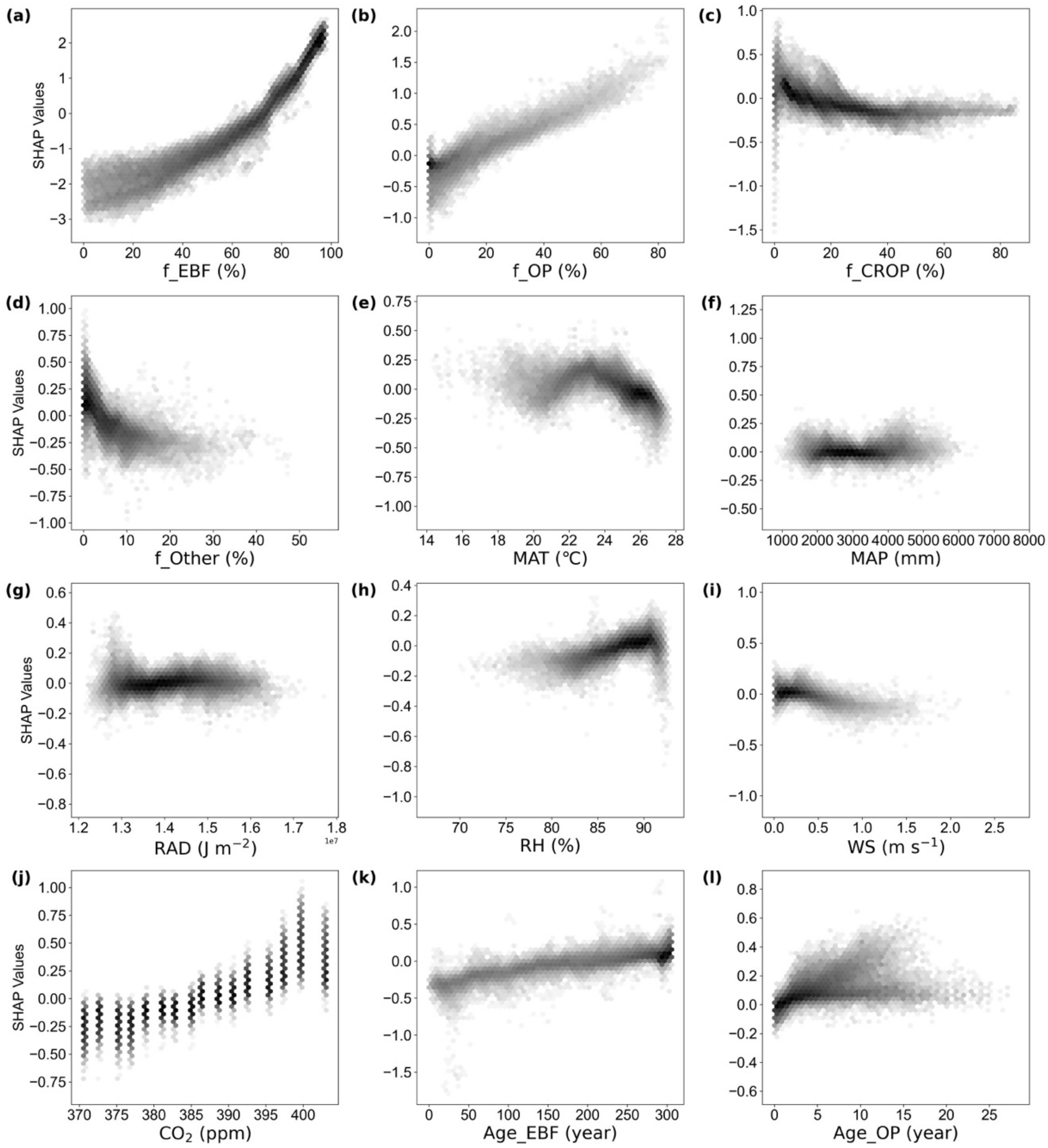

Figure S6: The density plots show the changes in SHAP values of each factor on LAI with corresponding factor variations. The abbreviations for each factor are available in Table S3.

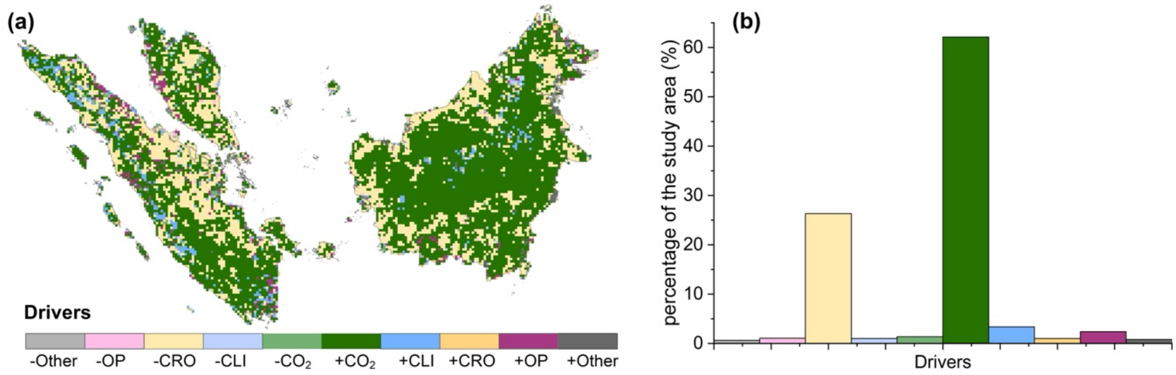

Figure S7: Spatial pattern of dominant drivers of trend in LAI (a), and the percentage of the study area dominated by each diver (b). The drivers include elevated CO_2 (CO_2), climate change (CLI), crop expansion (CRO), oil palm expansion (OP) and other land use changes (Other). A prefix '+' of the drivers indicates a positive impact on LAI trends, whereas '−' indicates a negative impact.

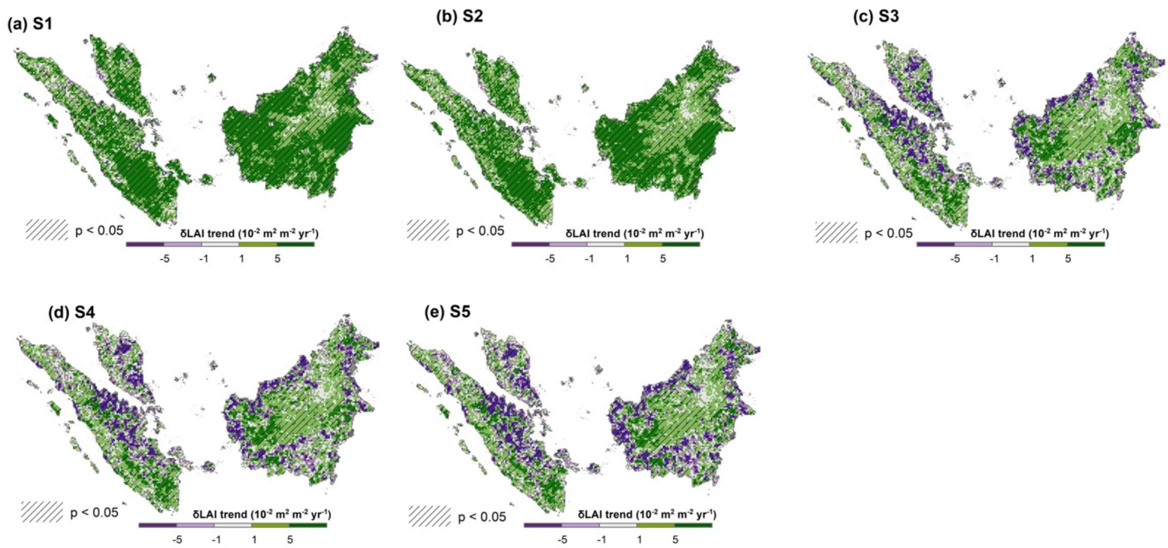

Figure S8: The spatial distribution of the pixel-wise impacts of each scenario on the greening trends. For S1, only CO2 concentration varied from 2001 to 2016, while climate and land use remained fixed at 2001 values. In S2, both CO2 and climate changed over time, but land use stayed constant. S3 to S5 progressively incorporated different land use processes: S3 considered EBF to CRO transitions with time-varying CO2, climate, and CRO fractions, while OP and other land uses remained constant; S4 added conversions from EBF to both CRO and OP; and S5 included all LUCC changes, with CO2, climate, and all land use types varying over time.

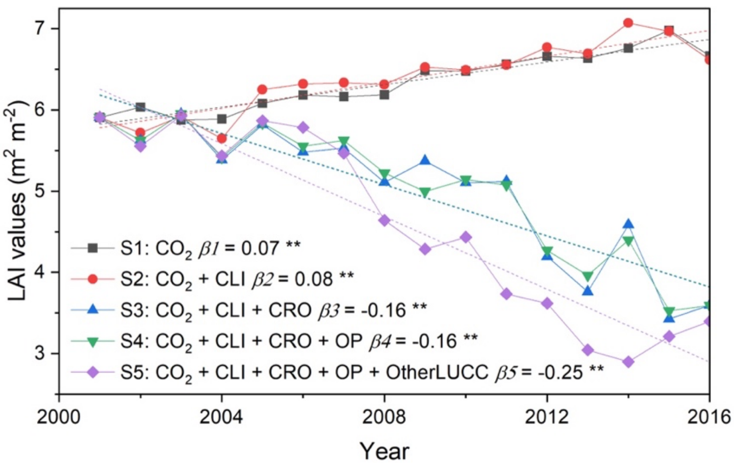

Figure S9: A selected pixel (102.15°E, 0.95°S) to show the gradual changes in prediction results for each scenario.

Table S1: The details of land use datasets in our study used to generate harmonized land uses in Southeast Asia.

Datasets	Time span	Spatial resolution	Sources
Global Forest Change maps (GFC)	2000-2022	30 m × 30 m	Hansen et al., 2013; https://glad.earthengine.app/view/global-forest-change
Land-use harmonization datasets (LUH2)	0850-2019	0.25° × 0.25°	Chini et al., 2021; https://luh.umd.edu/data.shtml
MODIS Land Cover Type Product (MCD12Q1)	2001-2000	500 m × 500 m	https://lpdaac.usgs.gov/products/mcd12q1v006/
Annual oil palm area dataset (AOPD)	2001-2016	100 m × 100 m	Xu et al., 2020; https://doi.org/10.5281/zenodo.3467071

Table S2: The annual fractions of each land use type in our study area from 2001 to 2016 (%).

Land Uses	2001	2002	2003	2004	2005	2006	2007	2008	2009	2010	2011	2012	2013	2014	2015	2016
EBF	73.41	72.67	71.92	70.83	69.76	68.57	66.97	65.46	63.77	62.82	61.66	59.84	58.67	57.01	55.84	53.09
CRO	14.45	14.69	14.94	15.57	15.81	16.37	16.97	17.57	18.53	19.13	19.80	20.82	21.50	22.53	23.31	24.56
OP	3.91	4.44	5.06	5.50	5.96	6.45	7.31	8.10	8.65	9.03	9.37	9.81	10.31	10.67	10.85	12.05
Pasture	3.20	3.20	3.04	3.01	3.24	3.30	3.38	3.44	3.51	3.49	3.55	3.73	3.68	3.78	3.84	3.98
Grass	0.63	0.64	0.62	0.62	0.65	0.66	0.67	0.67	0.69	0.70	0.71	0.74	0.74	0.76	0.77	0.79
Other Forest	0.08	0.02	0.02	0.03	0.04	0.07	0.04	0.04	0.04	0.02	0.02	0.03	0.03	0.04	0.04	0.03

Note: EBF, CROP, and OP are short for evergreen broadleaf forests, croplands, and oil palm plantations, respectively.

Table S3: The variables used to explain LAI variations using XGBoost model.

Categories	Variables	Descriptions and Units	Sources
Land use types	f_EBF	Fraction of evergreen broadleaf forest in the grid cell (%)	see Methods
	f_OP	Fraction of oil palm in the grid cell (%)	
	f_CRO	Fraction of cropland in the grid cell (%)	
	f_Other	Fraction of other land uses in the grid cell (%)	
Climate variables	MAT	Mean annual temperature (°C)	https://cds.climate.copernicus.eu/
	MAP	Total annual precipitation (mm)	
	WS	Wind speed (m s^{-1})	
	RAD	Shortwave downward radiation (J m^{-2})	
	RH	Relatively humidity (%)	
Stand Ages	Age_EBF	Stand ages of evergreen broadleaf forests (year)	https://doi.org/10.17871/ForestAgeBGI.2021
	Age_OP	Stand ages of oil palms (year)	http://dare.iiasa.ac.at/85/
CO_2 concentrations	CO2	Annual CO_2 concentrations (ppm)	https://gml.noaa.gov/dv/data/